



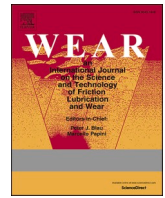
## **Coolant boiling and cavitation wear – a new tool wear mechanism on WC tools in machining alloy 718 with high-pressure coolant**

Downloaded from: <https://research.chalmers.se>, 2025-12-04 19:26 UTC

Citation for the original published paper (version of record):

Tamil Alagan, N., Hoier, P., Beno, T. et al (2020). Coolant boiling and cavitation wear – a new tool wear mechanism on WC tools in machining alloy 718 with high-pressure coolant. *Wear*, 452-453. <http://dx.doi.org/10.1016/j.wear.2020.203284>

N.B. When citing this work, cite the original published paper.



# Coolant boiling and cavitation wear – a new tool wear mechanism on WC tools in machining Alloy 718 with high-pressure coolant

Nageswaran Tamil Alagan<sup>a,\*</sup>, Philipp Hoier<sup>b</sup>, Tomas Beno<sup>a</sup>, Uta Klement<sup>b</sup>, Anders Wretland<sup>c</sup>

<sup>a</sup> Department of Engineering Science, University West, Trollhättan, Sweden

<sup>b</sup> Department of Industrial and Materials Science, Chalmers University of Technology, Göteborg, Sweden

<sup>c</sup> GKN Aerospace Engine Systems AB, Trollhättan, Sweden

## ARTICLE INFO

### Keywords:

Alloy 718  
Coolant boiling  
Cavitation wear  
High-pressure coolant  
Tool wear mechanism  
Tungsten carbide

## ABSTRACT

In recent years, research interest in liquid coolant media applied to the tool-workpiece interface (the tertiary shear zone) has grown considerably. In particular, attention has increased for work where the media has been applied under high-pressure. This is most likely triggered by the positive results reported on similar applications, but with coolant media directed towards the rake face of the cutting tool (the secondary shear zone). The most typical applications have not surprisingly been related to the machining of Heat Resistant Super Alloys (HRSA) or other “difficult to machine” alloys where the main intention has been to extend tool life and improve surface finish through reduced shear zone temperatures.

Concurrently, these achievements have revealed a knowledge gap and unlocked a new research area in understanding the effects and influences of coolant media applied on super-heated surfaces under high-pressure conditions. The aim of this study is to investigate the “coolant boiling and cavitation” phenomena that emerges during the application of coolant under high-pressure to the flank face of an uncoated WC tool while turning Alloy 718. The experimental campaign was conducted in three aspects: varying flank (coolant media) pressure; varying spiral cutting length (SCL); and varying cutting speed.

The results revealed that the location and size of the coolant-boiling region correlated with flank wear, coolant pressure and vapour pressure of the coolant at the investigated pressure levels. Further, the results showed that coolant applied with a lower pressure than the vapour pressure of the coolant itself caused the “Leidenfrost” effect. This then acts as a coolant media barrier and effectively reduces the heat transport from the cutting zone.

Further, erosion pits were observed on small areas of the cutting tool, resembling the typical signs of cavitation (usually found in much different applications such as pumps and propellers). The discovered wear mechanism denoted as “Cavitation Wear” was used as base for the discussion aimed to deepen the understanding of the conditions close to the sliding interface between the tool and the workpiece. Even though “Cavitation Wear” has been widely reported in hydraulic systems like pumps and water turbines, it is a new phenomenon to be seen on cutting tools while using high-pressure flank cooling.

## 1. Introduction

Use of coolant media is not only important to limit the impact from heat generated in the cutting process, but also an important means for chip transport. However, while in place and applied under high pressure, it will further improve the metal removing process. As such, high-pressure coolant assisted machining of Heat Resistant Super Alloys (HRSA) will inevitably be a technology aimed for the production lines of aerospace industries. The driver behind is improved tool life, better surface finish and increased chip break support enabling an increased

Material Removal Rate (MRR), thus, all in all a boost in productivity.

Alloy 718 is a widely used HRSA thanks to its excellent material characteristics, such as retained mechanical and thermal properties at elevated temperatures, low thermal diffusivity, hard abrasive carbides, improved creep and corrosive resistance as compared to other alloys. However, the same material characteristics lead to a poor machinability index [1]. Due to these properties, the heat generated in the cutting process is more prone to be transferred through the tool as compared to other alloys. Hence the accumulation of heat in the cutting edge causes high wear rates and significantly reduces tool life and MRR [2].

\* Corresponding author.

E-mail address: [nageswaran.tamil@hv.se](mailto:nageswaran.tamil@hv.se) (N. Tamil Alagan).

<https://doi.org/10.1016/j.wear.2020.203284>

Received 30 September 2019; Received in revised form 31 March 2020; Accepted 31 March 2020

Available online 11 April 2020

0043-1648/© 2020 The Authors. Published by Elsevier B.V. This is an open access article under the CC BY license (<http://creativecommons.org/licenses/by/4.0/>).

**Table 1**  
Terminology.

Terms	Explanation
Leidenfrost effect	When the liquid touches the heated surface, which is higher in temperature than the liquid's boiling point, it vaporizes immediately and forms an insulating vapour layer. This layer protects the remaining part of the liquid from boiling.
Zone 1	Flank wear area
Zone 2	No-coolant boiling area in between Zone 1 and Leidenfrost film.
Zone 3	Coolant boiling area below Leidenfrost film, presence of Cavitation wear (pits) identified.
Cavitation	The process of formation the vapour phase of a liquid when it is subjected to a reduced pressure at constant ambient temperature.

Other cooling methods for cutting tools such as pressurized air, Minimum Quantity Lubrication (MQL), liquid nitrogen (LN<sub>2</sub>) and carbon dioxide (CO<sub>2</sub>) assisted cooling may be considered, but the concept of high-pressure coolant is the most widely implemented cooling concept on production lines. None of the other cooling concepts have reached as far as high-pressure coolant assistance in terms of improved productivity. In particular, in the case of turning and with coolant jets directed to predefined target points in the vicinity of the cutting edge.

The physics involved in coolants directed to the cutting edge (high-temperature area) at elevated pressures is related to the creation of a hydro-mechanical force acting on the chip. But most important for this work is the formation of a hydraulic wedge between the tool and the workpiece that enables the heat transfer between the cutting edge and the coolant media.

The “static” energy of pressurized coolant media is transformed to “kinetic” energy that will create a bend and break-action on the chip. It will simultaneously reduce the heat generated through plastic deformation and frictional effects while the chip slides over the rake face (the secondary shear zone) and create better access for the coolant to reach the proximity of the cutting edge. The effect will be a reduction of the temperature of the cutting edge [3]. In our previous study, we have looked closer into this technology with the aim to better understand the physics behind the application of highly pressurized coolants, but also their impact on the thermal conditions of the cutting process. Investigations were undertaken to investigate if the additional application of coolant media would improve tool life and further lower the temperature in the cutting zone. Thus, the application of coolant at high-pressure directed towards the clearance/relief face of the tool (the tertiary shear zone), in addition to the high-pressure coolant that has already been applied to the rake face [4,5]. The results showed a significant improvement in tool life as compared to the “no flank cooling” conditions [6], and the application of high-pressure coolant led to the exploration of a new research area “Leidenfrost film and coolant-boiling”.

### 1.1. Coolant boiling and “Leidenfrost” effect in coolant assisted machining

The phenomenon of “coolant boiling” in machining with high-pressure coolant was recognized as early as 1952 by Pigott and Colwell [7]. They stated, “There appears to be an important cooling effect from the boiling oil as it reaches the edge; much more smoke and vapour are formed”. They identified that boiling is moderately critical at the vicinity of the cutting edge and decided to sweep the surface by high speed jets in order to lower the rate of boiling. In the last decades, several researchers have investigated the coolant-boiling phenomenon but with “different standpoints” as follows.

Few researchers stated the formation and existence of a vapour film acting as a barrier for the coolant to reach the vicinity of the cutting edge. Ezugwu and Bonney [8] reported that flood cooling was not an effective cooling strategy to lower the cutting temperature during machining of Alloy 718. The coolant vapourizes rapidly due to the

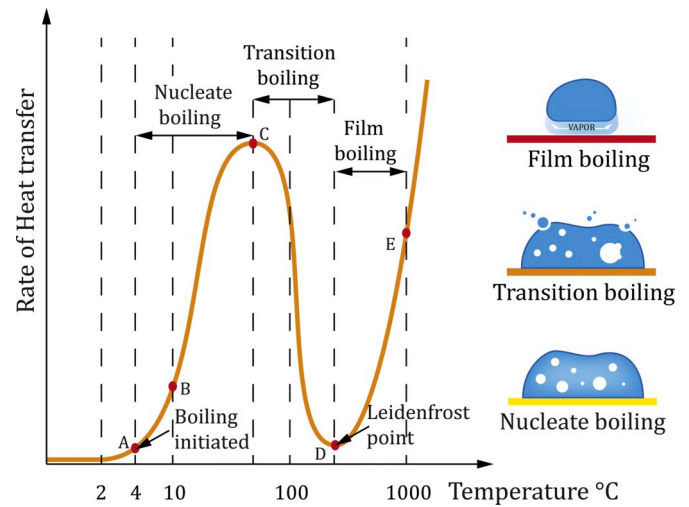


**Fig. 1.** Typical boiling curve for water at 1 atm, X-axis temperature represents the difference between excess surface temperature and saturation temperature of the fluid, adapted and reconstructed from Yunus A Cengel [13].

high-temperature close to the cutting edge and therefore cannot access the secondary and tertiary shear zone. Da Silva et al. [9] states that the overhead application of flood coolant led to boiling and immediate vapourizing, due to the high temperature in the primary shear zone; hindering fresh coolant to access the hot parts of the cutting edge. This has a negative effect on the heat transfer rate. To eradicate this problem and improve cooling, the solution was to apply the coolant at high-pressure, thus eliminating the vapour that appears close to the hot regions of the cutting edge. The vapour problem was “deciphered” by high-pressure coolant, but the investigation was not focussed on the physics behind the application of high-pressure coolant and related coolant boiling.

Kramer et al. [10] also noticed “coolant boiling” and investigated the vapour bubble theory in machining Ti6Al4V with high-pressure coolant. The authors stated that the boiling of the cutting fluid forms a firm vapour bubble close to the cutting edge that prohibits the cold fluid from reaching the cutting edge. Based on the relation between cutting tool temperature, steam and coolant pressure, and the flow rate established to lower the tool temperature, it is important to increase the coolant pressure but not necessarily with an increase of the flow rate for a constant pressure.

Klocke et al. [11] postulated the vapour barrier theory and investigations were carried out by supplying the coolant at high-pressure to break the vapour barrier for effective cooling and increased tool life. However, there is still a knowledge gap in the understanding of this phenomenon.

Jäger et al. [12] explained the vapour barrier theory as the “Leidenfrost” effect. This effect was discovered by J. C. Leidenfrost in 1756 [13]. When the liquid touches the heated surface, which is higher in temperature than the liquid's boiling point, the liquid vapourizes immediately and forms an insulating vapour layer. This layer protects the remaining liquid from boiling and is known as the “Leidenfrost” effect. The vapour film has lower thermal conductivity than the liquid. In Fig. 1, the curve of water boiling is illustrated, where the temperature (x-axis) represents the difference between excess surface temperature and saturation temperature of the fluid.

Point A is the point at which boiling is initiated. Once the temperature increases into the region of B–C, which is above the saturated fluid temperature and typically in the case of water, the range is between 10 and 30 °C, the formation of bubbles increases with the number of nucleation sites in the liquid. This leads to the formation of several continuous columns of vapour, which subsequently rises to the free surface at higher rates to release their vapour content.

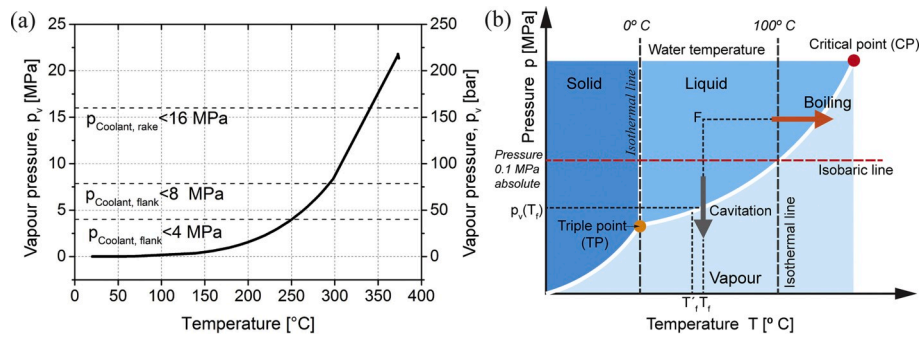


Fig. 2. (a) Influence of temperature on vapour pressure of water adapted and reconstructed from Sorby and Tonnessen [15]. (b) Thermodynamic phase diagram of water redrawn from Franc and Michel [16].

Point C exhibits the maximum heat transfer rate. The nucleate boiling regime is a desired type of boiling in the aspect of heat transfer rate. Further increase in temperature leads to the region of C-D, transition boiling, where the heat transfer rate starts to decrease due to the coverage of the heated surface by the vapour film. In addition, both nucleate and film boiling occurs simultaneously in the transition regime.

Further increase in temperature leads to point D, the so called *Leidenfrost* point, where the heat transfer rate is at its lowest level due to the protecting vapour film. This film can be removed by an additional increase in temperature leading to radiation effects [13].

Tamil Alagan et al. [14] investigated the *Leidenfrost* effect on textured cutting tools. The cutting tools with an increased surface area and channel design aimed to increase heat transfer rate. The tools were subsequently tested under both rake and flank cooling conditions. Results showed that textured cutting tools improved the heat dissipation rate and reduced the flank wear rate, even without the flank cooling. Furthermore, energy-dispersive x-ray spectroscopy (EDS) results showed no traces of “coolant boiling” in the form of strong calcium precipitates. However, calcium (Ca) precipitates were observed on the flank surface for non-textured tools at standard cooling conditions. This shows that the textured tool in combination with high-pressure cooling improved the heat dissipation rate and also influenced the *Leidenfrost* film.

As stated by Klocke et al. [17], the vapour pressure of the boiling coolant opposes the pressure of the coolant jet at the coolant-vapour interface. In order to avoid the formation of a vapour barrier, it is necessary for the coolant pressure to exceed the vapour pressure at the present temperature [15]. The increase of vapour pressure with temperature is shown in Fig. 2 (a). For any given temperature at the tool

surface, it is possible to estimate the minimum required coolant pressure necessary to suppress the formation of a vapour barrier, see Fig. 2 (b). Thus, to avoid the limiting effects from the *Leidenfrost* film, it is important to control the cutting temperature with respect to the coolant’s nucleate boiling temperature. Otherwise, in order to maintain an efficient heat transfer, the pressure with which the coolant is applied to the hot surface must be raised above the vapour pressure of the coolant for that specific temperature.

### 1.2. Cavitation wear – theory, types and stages

Research regarding cavitation wear is most commonly conducted with respect to turbines, pumps, propellers etc. where the isothermal and isobaric conditions are the main parameters of the investigation. The connection between cavitation and high-pressure coolant assisted machining is explained at the end of this section with the reason for the experimental investigation. The following paragraph is an introduction to this wear mechanism and intended as a “walkway” to the understanding of this phenomena.

In the 1950’s, Eisenberg [18] defined cavitation as “the process of formation the vapour phase of a liquid when it is subjected to a reduced pressure at constant ambient temperature”. It can be related to the boiling process of the liquid due to the pressure reduction instead of the heat addition. Boiling of a liquid may occur through an increase of the vapour pressure or a decrease of the atmospheric pressure, see Fig. 2 (b). The basic physical and thermodynamic processes are the same in both cases. However, the liquid is said to cavitate – to form vapour bubbles – and make them grow because of the pressure reduction.

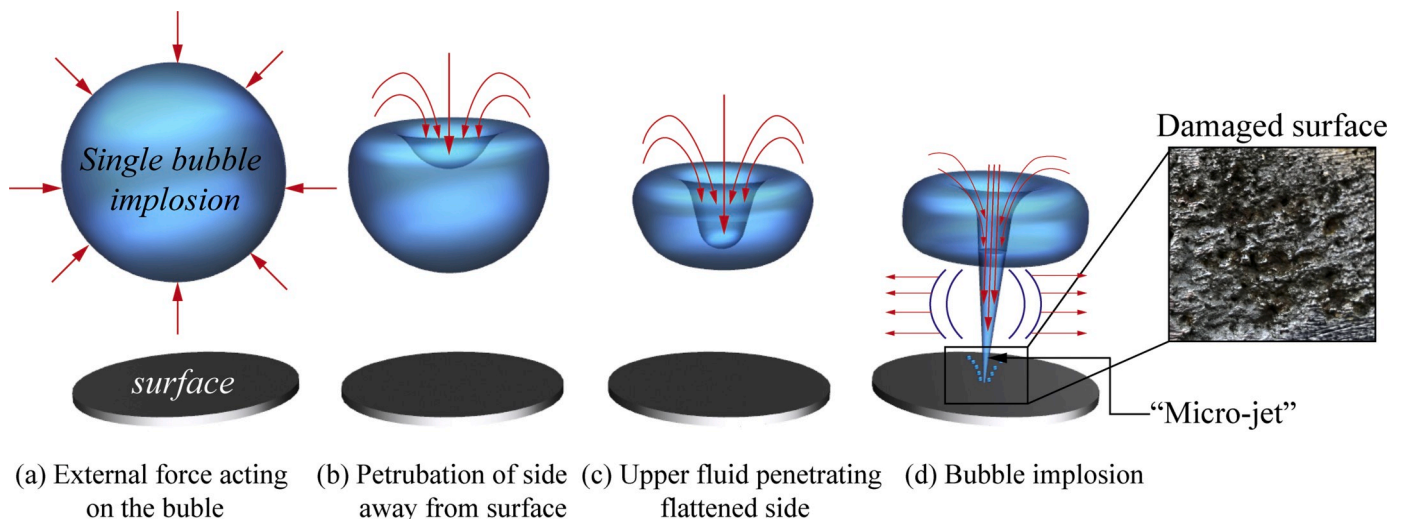


Fig. 3. Formation and collapsing of vapour bubble – cavitation/micro jet mechanism adapted and reconstructed from Brennen and Ronald [24,25].



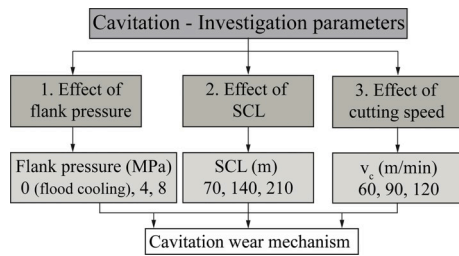


Fig. 4. Overview of the research methodology incorporating investigated parameters focussed on cavitation wear.

The phase diagram of water is illustrated in Fig. 2 (b). The interesting part is the curve between the triple point (TP) to a critical point (CP) which separates the liquid and vapour phase. For instance, crossing the TP-CP curve represents a reversible transformation under static or equilibrium conditions as a function of temperature, i.e. evaporation or condensation of the liquid at pressure  $p_v$ , the vapour pressure. Similarly, at a constant temperature, lowering the pressure can cause cavitation to appear in a liquid. Thus, cavitation is similar to boiling except that the driving mechanism is different. It is to be noted that in some cases, the heat transfer needed by vapourization to change the phase occurs at  $T$ , which is lower than  $T$ . This difference in temperature is called “thermal delay” in cavitation [16,19].

Cavitation occurs as the local field pressure approaches the saturation pressure of the fluid, which initiates the evaporation process causing the cavitation nuclei to grow to vapour filled “cavitation bubbles”. Once the pressure inside the bubbles exceeds the surrounding field pressure, the bubbles will collapse and condense (i.e. the physical state changes from liquid to vapour and then back to liquid) [20,21].

Fitch [21] distinguished between two types of cavitation: gaseous and vaporous. Gaseous cavitation is a diffusion process, occurring when the static pressure falls below the saturation pressure of the non-condensable gas dissolved in the liquid. This effect generates a lot of

noise, high temperatures, molecular level cracking and degrades the chemical composition of the fluid through oxidation. It is a much slower process as time depends on the conversion rate (fluid circulation). However, most importantly, gaseous cavitation does not erode the surface of the material. Thus, the vaporous cavitation is the phenomenon of interest in this context as it gives rise to a “fluid to surface” type of wear. A portion of the liquid is initially exposed to tensile stresses, which causes the liquid to boil. Immediately thereafter, it is exposed to compressive stresses, which causes the vapour bubbles to collapse (i.e. to implode) [21]. Fig. 3 depicts bubble collapse generating mechanical shock which causes a “micro-jet” by unifying the liquid to impinge against the surfaces. Wiggert et al. [22] stated: “vaporous cavitation takes place if the bubble grows explosively in an unbounded manner with rapid phase change of a liquid into vapour”. This type of cavitation occurs rapidly in microseconds and erodes the surface causing cavitation wear. Multiple terms are widely used to represent cavitation: cavitation pitting, vaporous cavitation, cavitation erosion, cavitation fatigue, liquid impact erosion, etc. [22,23].

Findings from the investigation of the coolant boiling region on the flank face of the cutting tools with high-pressure coolant assisted machining, revealed the presence of “eroded pits” [26]. In the present paper further investigations were conducted on the effect of coolant boiling and movement of “Leidenfrost” film with varying flank pressure conditions which led to these eroded pits being formed due to “Cavitation Wear”. Therefore, careful examination of coolant boiling, the Leidenfrost effect and cavitation wear have been performed. Further, it is discussed how the eroded pits are related to high-pressure coolant assisted machining as well as the experimental findings on the existence of the “Cavitation Wear” as a new tool wear mechanism.

## 2. Experimentals

The experimental investigation of cavitation wear was framed with the intention to be arbitrary, see Fig. 4. That led to three different sets of conditions as tabulated in Table (2–4).

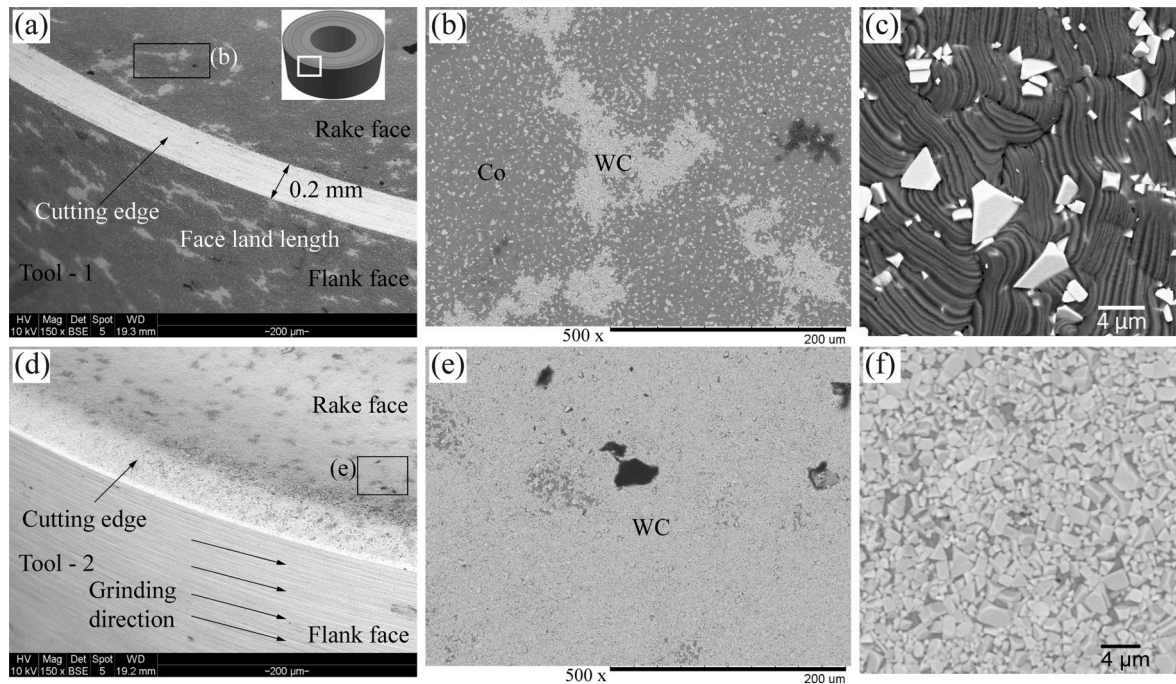


Fig. 5. (a–c) BSE micrographs of Tool-1: (a) Cutting edge including the face land (location of image shown in insert); (b) Higher magnification of the rake face of Tool-1; (c) Detail of the “Co-capping layer” covering the tool surface - the dark phase is the Co-binder and the bright particles are WC grains. Fig. 5(d–f) BSE micrographs of Tool-2: (d) The cutting edge including the face land of Tool-2 shows the grinding direction; (e) Higher magnification of the rake face; (f) Mapping of WC as bright particles.

In theory, formation of cavitation wear is physically possible when there is a pressure difference. This brings out the first set of experiments where the flank pressure conditions are varied (0 means no coolant applied at an elevated pressure i.e. flood cooling, 4 and 8 MPa).

- The intention of the first test campaign is to investigate the impact of pressurized coolant with reference to flood cooling.

The second set of experiments was focused on constant coolant conditions but varying the spiral cutting length, SCL, (essentially proportional to the progression of tool wear during a continuous machining sequence), which leads to an increase of the machining time and the amount of material removed.

- The intention of the second test campaign is to investigate the effect of cavitation for increased SCL (in fact increased flank wear).

The third set of experiments was focused on varying the cutting speeds to observe how increased heat related to cutting speed influences cavitation.

- The intention of the third test campaign is to investigate the effect of cavitation for increased temperature (in fact increased cutting speed).

### 2.1. Cutting tool description

Carbide tools are comparably cost effective and easily available from several sources. In rough machining, round cutting tools play a vital role while machining HRSA, due to their excellent edge strength and the fact that one insert can be used for several but varying geometric cutting conditions during one and the same cut (pass). This is of particular interest while machining curved shapes.

Round uncoated cemented carbide inserts with the ISO designation RCMX 12 04 00 were used in the test campaign. Since the cutting tools (inserts) do constitute a vital part in the investigation of the coolant boiling phenomenon (acting as detectors), their surface constitution is an important part of the evaluation process. Thus, a careful examination of the surface properties of commercially available tools (inserts) was performed. This was important that a typical flank surface of an insert is ground in order to maintain a high degree of geometrical accuracy. However, this might not necessarily be ideal for the detection of coolant boiling.

An insert with a thin layer of cobalt ("Co-capped layer") was chosen. For the present investigation, this was considered particularly advantageous since such layer provides for that constant thermal conductivity properties of the tool surface can be assumed. In addition, pre-emptive tests showed that the smooth "Co-capped" surface made the evaluation process easier. In particular, adherence of the coolant precipitates on the flank face of the insert while doing ordinary LOM investigations, even though the main advantage with the "Co-capped" surface with respect to its analysing properties became apparent during the SEM investigations.

A ground insert with similar designation was chosen for reference and used for a reduced set of tests.

The inserts chosen were commercially available, which was considered an advantage for the investigation since a continuous and robust production process enables high confidence in the obtained test results. The inserts were supplied by two independent cutting tool manufacturers.

The tools (inserts) were designated Tool-1 (cobalt on the surface referred to as "Co-capped layer") with an average hardness of  $1545 \pm 14$  HV30 and Tool-2 (no cobalt on the surface) with an average hardness of  $1563 \pm 6$  HV30. The inserts were made of uncoated sintered carbide consisted of 95% tungsten carbide (WC) and 5% cobalt (Co) as binder.

**Table 2**

Cutting parameters for face turning Alloy 718 with different flank pressure conditions (Tool-1).

Parameter	Value
Inserts	Tool-1
Spiral cutting length, SCL, m	90
Feed rate, $f_n$ , mm/rev	0.2
Depth of cut, $a_p$ , mm	1
Material removed, MR, $\text{cm}^3$	18
Cutting speed, $v_c$ , m/min	45
Machining time, $t_m$ , s	120
Machined length, $l_m$ , mm	8
Rake pressure, RP, MPa	16
Flank pressure, FP, MPa	0, 4, 8

### 2.2. Machine setup, workpiece material, cutting and high-pressure coolant conditions

A 5-axis vertical CNC machine was used for a face turning operation of a cast Alloy 718 ring with an average hardness of  $381 \pm 21.8$  HV. The machine was programmed for constant cutting speed (spindle speed proportional to the radial position of the tool). High-pressure coolant was supplied to both rake and flank face. This was done through a specially designed tool holder with three nozzles pointing towards the rake side of the insert, each with a diameter of 0.8 mm. The tool holder was also equipped with two nozzles pointing towards the relief side of the tool, each with a diameter of 1.2 mm. The precise focus of the coolant jets was set to be just behind the rim of the cutting edge. The tool holder and coolant impact points can be seen in Ref. [6]. The machining setup is provided in Ref. [14]. An emulsion of 5% concentrate mixed with water at room temperature was used as coolant media. The Spiral Cutting Length, SCL, is calculated from Eq (1), where  $D_m$  is the machined diameter,  $D_1$  the initial diameter and  $l_m$  the (approx.) machined length. The corresponding outer and inner diameters of the Alloy 718 ring are 742 and 672 mm, respectively [14].

$$SCL = \left[ \frac{D_1 + D_m}{2} \right] \times \left[ \frac{\pi}{1000} \right] \times \left[ \frac{l_m}{f_n} \right] \quad (1)$$

Based on the research methodology, see Fig. 4, three sets of experiments were carried out to investigate the tools with respect to coolant boiling and the *Leidenfrost* effect for closer examination of the cavitation wear mechanism. The cutting tool of primary interest was Tool-1 due to the smooth surface of the relief surface (due to "Co-capping"), in order to minimize any interference with the "hydrodynamic surfaces" of interest for the investigation. The experiments were conducted in randomized order to avoid systematic errors.

#### Test 1:

The first set of experiments was designed for Tool-1 by varying the flank pressure conditions (0, 4 and 8 MPa) while the other cutting parameters were held constant, see Table 2. Every cutting condition was replicated two times, to ensure repeatability.

#### Remark:

- In addition to the first test series, several "coolant impingement tests" were conducted to investigate the tool surface and the effect of cavitation without machining. For this purpose, new cutting tools were subjected to high-pressure cooling with the same coolant supply pressures (16 MPa rake face cooling and 8 MPa flank face cooling) placed in the tool holder, but without concurrent machining. The tests were conducted with increasing exposure times (1, 2, 5, 10 and 20 min).

**Table 3**

Cutting parameters for face turning Alloy 718 with different SCL conditions for (Tool-1).

Parameter	Value
Insert	Tool-1
Cutting speed, $v_c$ , m/min	60
Feed rate, $f_n$ , mm/rev	0.2
Depth of cut, $a_p$ , mm	1
Rake pressure, RP, MPa	16
Flank pressure, FP, MPa	8
Machined length, $l_m$ , m	6.1, 12.4, 18.5
Spiral cutting length, SCL, m	70, 140, 210
Machining time, $t_m$ , s	70, 140, 210

**Table 4**

Cutting parameters for face turning Alloy 718 with different cutting speeds (Tool-1 and Tool-2).

Parameter	Value
Inserts	Tool-1 and Tool-2
Spiral cutting length, SCL, m	60
Feed rate, $f_n$ , mm/rev	0.3
Depth of cut, $a_p$ , mm	1
Material removed, MR, $\text{cm}^3$	18
Machined length, $l_m$ , mm	8
Rake pressure, RP, MPa	16
Flank pressure, FP, MPa	8
Cutting speed, $v_c$ , m/min	60, 90, 120
Machining time, $t_m$ , s	60, 40, 30

### Test 2:

The second set of experiments using Tool-1 was designed to understand the effect of coolant boiling and cavitation by increasing the SCL/cutting time without alteration of the coolant pressure nor the cutting conditions, see Table 3. The test with the shortest SCL was conducted three times in order to ensure repeatability of the obtained results.

### Test 3:

The third set of experiments was planned for different cutting speeds (to increase the cutting temperature) for Tool-1 (with a “Co capped” surface). In addition, to verify the performance of the “Co-capped” tool as detector of *coolant boiling* and *cavitation wear*, through a “back to back” test with Tool-2 (no “Co capped” surface). In both experiments, the total material removal was kept constant ( $18 \text{ cm}^3$ ), see Table 4. Also, for these tests, all cutting conditions were replicated at least two times to ensure repeatability.

## 2.3. Characterization

For the round insert, a procedure for how to define the depth of cut line and the corresponding wear land had to be established [14]. Tool wear investigations were conducted by different methods. Both Light Optical Microscope (LOM), and 3-D scanning microscope based on the Infinite Focus variation technology [27] was used for maximum and average flank wear and flank wear area calculations. The measurement of the maximum width of the flank wear land was conducted based on the ISO 1993:3685 standard [28]. In addition, the flank wear area was calculated for some of the tools for a better understanding of the wear zone [6]. New tools as well as worn flank faces from the conducted tests, were studied in a Scanning Electron Microscope (SEM), making use of both Back-Scatter Electrons (BSE) and Secondary Electrons (SE) imaging. Furthermore, Energy-Dispersive X-Ray Spectroscopy (EDS) was applied for qualitative chemical analysis (element mapping).

## 3. Results and analysis – tool wear investigation – cavitation wear

### 3.1. Varying flank pressure on Tool-1

The Tool-1 surface prior to tests can be seen in Fig. 5 (a), where the cutting edge of a new tool with rake and flank face is shown. The higher magnification micrograph in Fig. 5 (c) reveals the presence of the Co-binder on the surface which can be recognized as the dark phase with stepped appearance. Accumulation of Co-binder, also known as “Co-capping” [29,30], was found on the entire surface of the tools except for the face land and is commonly observed on carbide tools. The formation of “Co-capping” during liquid phase sintering is discussed elsewhere [29,30].

The research aim was to investigate the coolant pressure conditions on the flank face of the tool, in order to correlate the coolant boiling region (due to heat) with the flank wear. The use of coolant on the high-temperature shear zones leads to formation of the *Leidenfrost* film, which prohibits the coolant to reach the cutting edge and further to create a coolant boiling region below this film. Such conditions are typical for machining HRSA materials such as Alloy 718 where the heat is sealed in the cutting zone and increases drastically with respect to machining time. By using coolant at high-pressure, in this case at 8 MPa, the tool wear was lowered and in addition moved the *Leidenfrost* film and the coolant boiling region closer to the cutting edge. This was also the case for the flank wear, which was lower in a similar pattern as compared to the “no flank pressure condition”, see Fig. 8. These findings align with the previous research work and the work of the authors stating that the high-pressure coolant can improve the heat dissipation and influence the coolant boiling. Hence, coolant applied at high pressures can suppress the vapour film [6,15,17].

Further SEM examination of the coolant-boiling region was

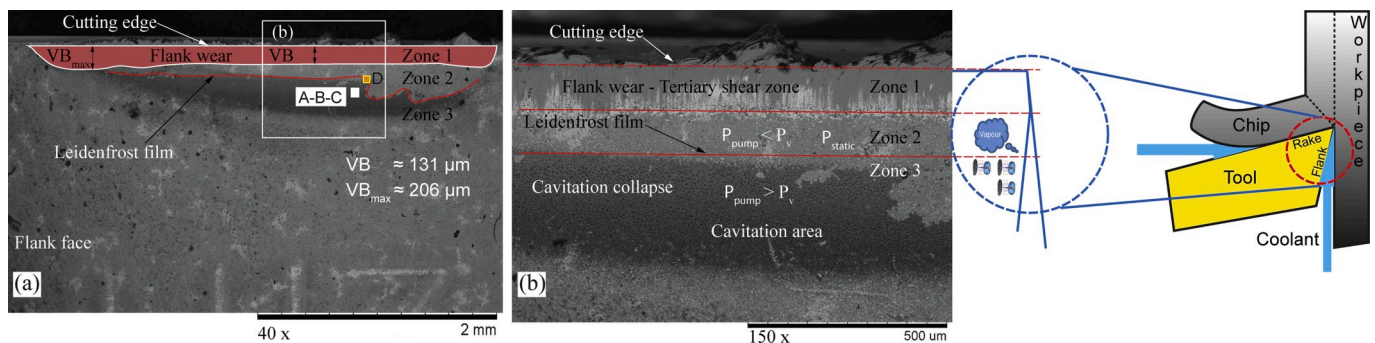


**Fig. 6.** SEM micrograph of Tool-1 machined Alloy 718 at  $v_c$  45 m/min,  $f_n$  0.2, rake pressure 16 MPa and flank pressure 4 MPa: (a) Flank face illustrating 3 different zones; (b) higher magnification image of the zones and cavitation area.



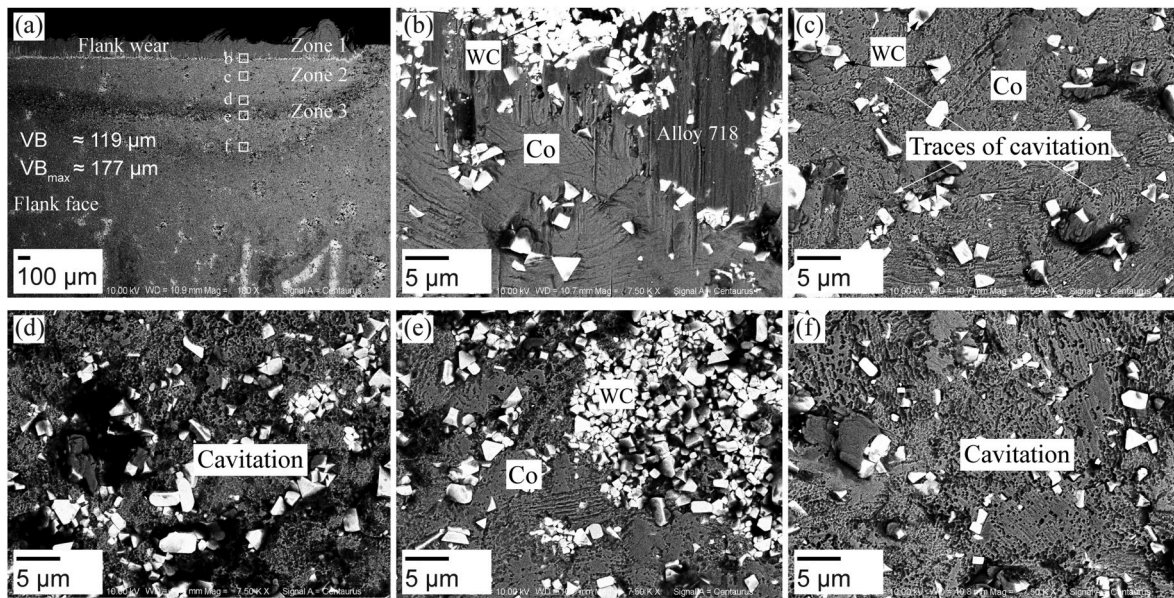


**Fig. 7.** BSE micrographs of Tool-1 machined Alloy 718 at  $v_c$  45 m/min,  $f_n$  0.2, rake pressure 16 MPa and flank pressure 4 MPa: (a) flank face illustrating 3 different zones; selected areas on higher magnification: (b) border of Zone 1 and 2, (c) Zone 2, (d) border of Zone 2 and 3, (e) Zone 3, and (f) further away from Zone 3.

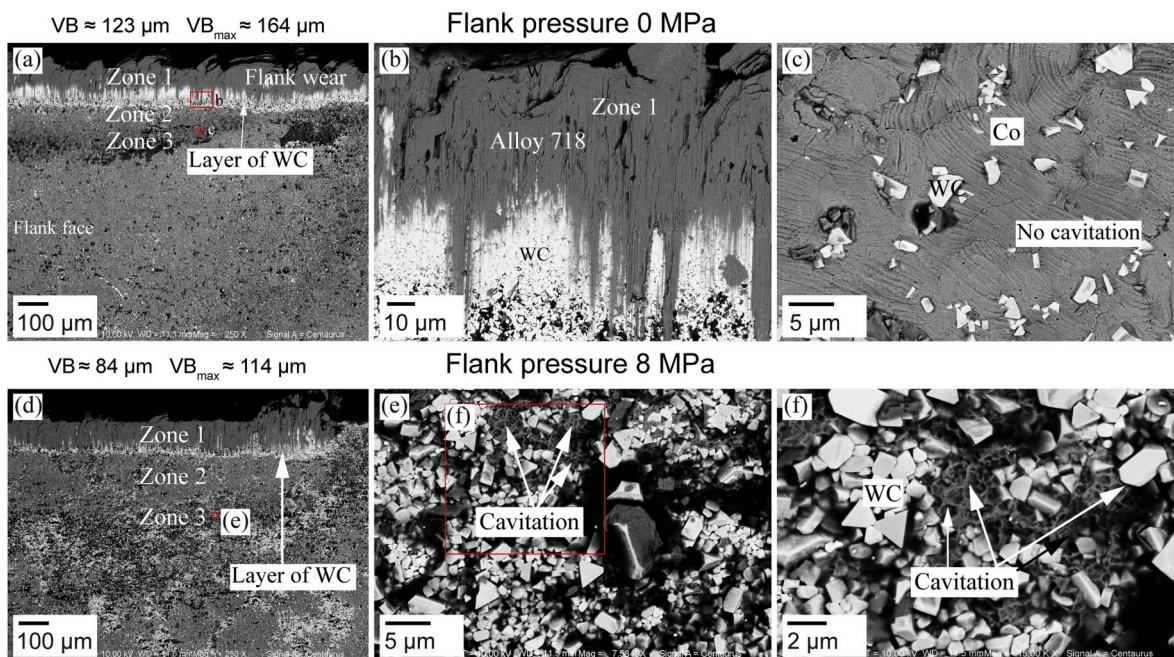


**Fig. 8.** BSE micrographs of flank faces of Tool-1 used for machining Alloy 718 at  $v_c$  45 m/min,  $f_n$  0.2, rake pressure 16 MPa, (a–c) no flank cooling, (d–f) flank pressure of 8 MPa (b) Zone 1 flank wear area (c) Zone 3 no trace of cavitation (e) Zone 3 coolant boiling region with signs of cavitation (f) higher magnification of Zone 3 showing the cavitation on the cobalt region.

conducted on Tool-1. This tool was used to machine Alloy 718 with a rake pressure of 16 MPa and flank pressure of 4 MPa at a  $v_c$  of 45 m/min. Based on the understanding of the *Leidenfrost* and the coolant boiling effect, the flank surface of Tool-1 was categorised into three different regions to be investigated in detail: Zone 1, 2 and 3, see Fig. 6 (a). In addition, Fig. 6 (a) illustrates expected location of the points (A–D) from the boiling curve, see Fig. 1.

Zone 1 is the area of contact in the tertiary shear zone where abrasive flank wear occurs due to interaction between the tool and the workpiece material. The wear rate increases due to work hardening, the presence of carbides and the poor thermal conductivity of Alloy 718 that leads to a

drastic increase of the cutting tool temperature. High-pressure coolant is used to extract heat and improve the tool life. However, the high tool temperature leads to rapid coolant vapourizing, which immediately forms the *Leidenfrost* film. This film acts as a barrier prohibiting the coolant to reach the proximity of the cutting edge. Hence, forming Zone 2 (no-coolant boiling) between Zone 1 and the *Leidenfrost* film see Fig. 6.

The dark area seen below the *Leidenfrost* film is Zone 3 (coolant boiling) see Fig. 6, and was established from EDS analysis in our previous investigations to be coolant residues i.e. calcium precipitates [12].

When investigating Zones 2 and 3 with respect to the applied pressure (seen in Fig. 6 (b)), it is clear that the *Leidenfrost* film does not only



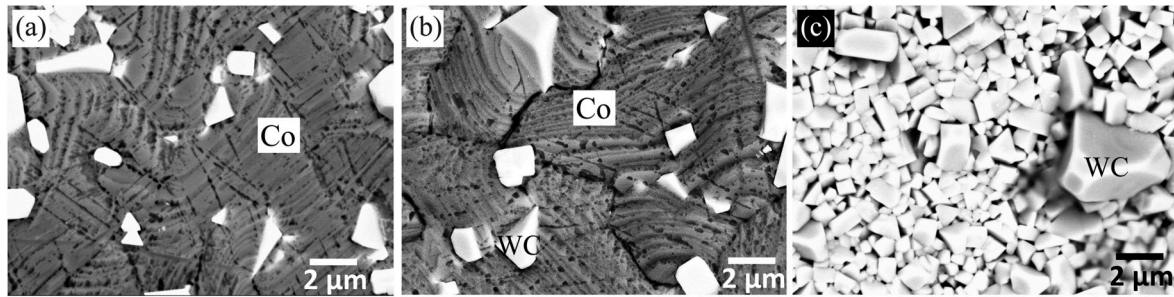


Fig. 9. BSE images of erosion obtained after (a) 16 MPa coolant impact for 20 min, (b) 8 MPa coolant impact for 20 min (both without concurrent machining), and (c) 8 MPa coolant impact for 3.5 min while concurrent machining.

prohibit the coolant to access the hot region, but likely creates a pressure difference in Zone 2 and 3. Zone 2 is expected to have high temperature since the coolant cannot access this area and coolant pressure is lower than the vapour pressure (due to the temperature). In Zone 3, the temperature is expected to be lower as compared to Zone 2, due to the coolant interaction on the hot surface.

Based on these conditions, it can be stated that between Zone 2 and Zone 3 there exists a temperature/pressure difference due to the *Leidenfrost* film. This leads to the formation of vapour bubbles in the liquid and their collapse on Zone 3 where the pressure is supposed to be higher than in Zone 2. It should be noted that in vapour cavitation, the coolant temperature is a vital parameter since the vapour pressure depends on the coolant temperature and governs the cavitation effect [21].

Fig. 7 depicts SEM micrographs of Tool-1 focussed on different zones. Fig. 7 (a) illustrates the three different zones: Zone 1 – flank wear, Zone 2 – no coolant-boiling and Zone 3 coolant-boiling. Fig. 7 (b) focusses on the margin between Zone 1 and 2 where workpiece material Alloy 718 adheres to the flank wear region as well as the cobalt region. Fig. 7 (c) shows selected area on Zone 2, where Co can be found and small signs of cavitation pits. Fig. 7 (d) shows the border region between Zone 2 and 3 the coolant boiling region, due to the *Leidenfrost* film is likely creating pressure/temperature difference, thus clearly showing the existence of “Cavitation pits” on the cobalt area. Fig. 7 (e) shows a selected area on Zone 3, away from the *Leidenfrost* film with fewer signs of cavitation pits and more WC visible as compared to Fig. 7 (d). Fig. 7 (f) was obtained even further away from the boiling region and nevertheless shows signs of cavitation.

The cavitation pits can be correlated to the findings of Finch [21] that the implosion of the vapour bubbles generates high-intensity pressure, which in microseconds (speed of sound) can create a *micro-jet*, shock wave and noise. The shock waves that occur can drastically increase the pressure up to ~685 MPa (100,000 psi) at the point of collapse and a very high local temperature is created at the surface of the bubble for a short time. The repeated and imminent implosion of the vapour bubbles can cause serious damage to the surface in terms of micro pits on the surface. This phenomenon is called the “Cavitation” [21,31], see Figs. 6 (b), Fig. 7(c–f).

To further understand the coolant boiling and the cavitation effect, machining was conducted with no flank pressure cooling (0 MPa). The corresponding SEM micrographs of tool flank face are shown in Fig. 8 (a–c). In theory, when not using the high-pressure coolant, the absence of a strong coolant barrier in the form of *Leidenfrost* film, higher flank wear and no cavitation is to be expected, since there will be no possibility to create a pressure difference. The experimental results from the flank face of the tool showed higher flank wear and some areas of boiling as dark region.

It is to be noted that the condition of “no flank cooling” means there is no application of coolant at a pressure. However, the coolant used at the rake and flood cooling from the tool holder will have access in the tertiary shear zone. This could cause the coolant to leave residues on the tool flank surface in the form of the dark region.

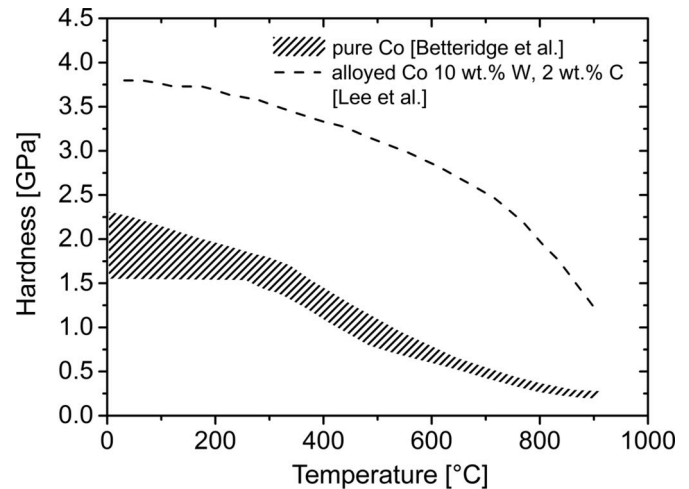
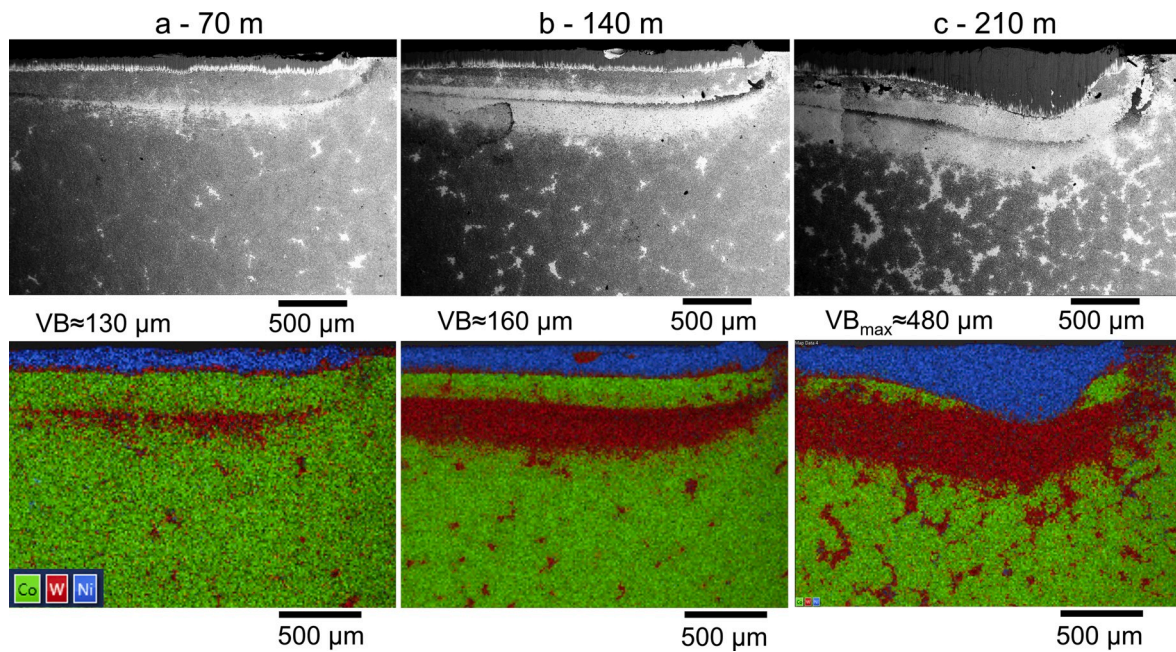


Fig. 10. Reported high-temperature hardness data of pure Co and Co alloyed with W and C, adapted from Betteridge and Lee [33,34].

In Fig. 8 (b), a selected area in the region of Zone 1 and 2 shows the adherence of Alloy 718 and the clear visibility of WC. Most importantly in Fig. 8 (c), we could not see any sign of cavitation on the tool. The result shows that “no coolant pressure” on the flank leads to an increase in flank wear. In addition, “no cavitation wear” was observed and “cavitation wear” is not related to increased flank wear. On the contrary, Fig. 8 (d) shows the SEM micrograph of the tool machined with flank cooling at 8 MPa illustrating the three zones. The selected area of Zone 3 in Fig. 8 (e) shows mainly the presences of WC (white regions). In between the WC, “cavitation pits” are visible on the cobalt at higher magnification in Fig. 8 (f). These results show that the coolant pressure decreases the flank wear.

The *Leidenfrost* film acts as a barrier that prohibits the coolant to access the tool and causes the pressure difference that could lead to the cavitation wear mechanism. The WC has higher hardness than Cobalt. Hence, the *micro-jet* created is in this case high enough to generate cavitation pits in the weaker and softer Co phase.

To verify the “cavitation wear/pits” phenomenon, cutting tools were tested by impinging high-pressure coolant on the tool rake and flank surface without machining. The pits observed in high-magnification SEM micrographs were far smaller or even negligible as compared to the cutting tools after machining tests. This is exemplified in Fig. 9 (a and b) where the tool surfaces after 20 min exposure to high-pressure cooling with 16 and 8 MPa on the rake and flank surface, respectively, is shown. Some pits have formed in the Co-binder and their morphology and size was found to be similar for both coolant supply pressures to the rake (16 MPa) and the flank (8 MPa). Even though the coolant exposure time was significantly longer than during the machining tests, no substantial removal of Cobalt occurred and the WC grains were not exposed



**Fig. 11.** BSE micrographs of flank faces of the worn tools after the tests stopped at spiral cutting lengths of (a) 70 m, (b) 140 m, and (c) 210 m. The upper row shows the BSE micrographs and the lower row the corresponding EDS maps. Elemental distribution of Co is given in green, W in red, and Ni in blue. (For interpretation of the references to colour in this figure legend, the reader is referred to the Web version of this article.)

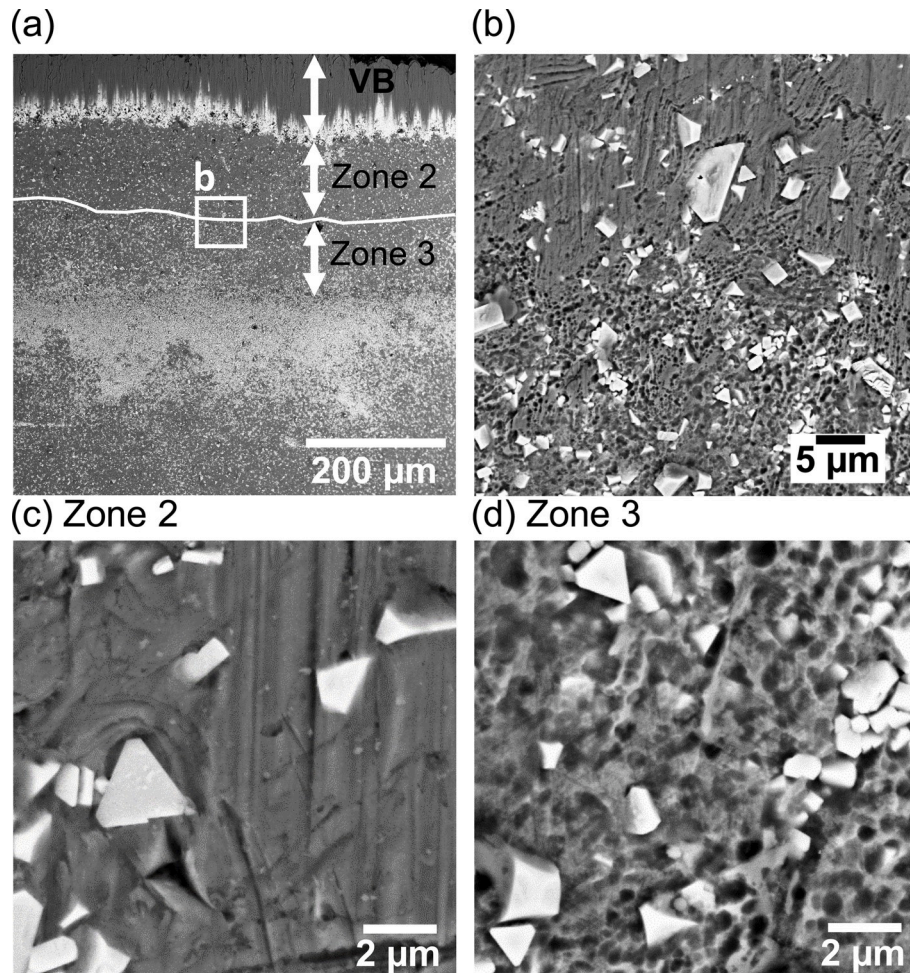


**Fig. 12.** BSE images of the tool surface below the flank wear land (VB) after 70 m spiral cutting length: (a) overview of flank face with zones of distinct features indicated. Higher magnified views of the Co-capping layer: (b) at the interface between Zone 2 and 3, (c) in Zone 2, and (d) in Zone 3.



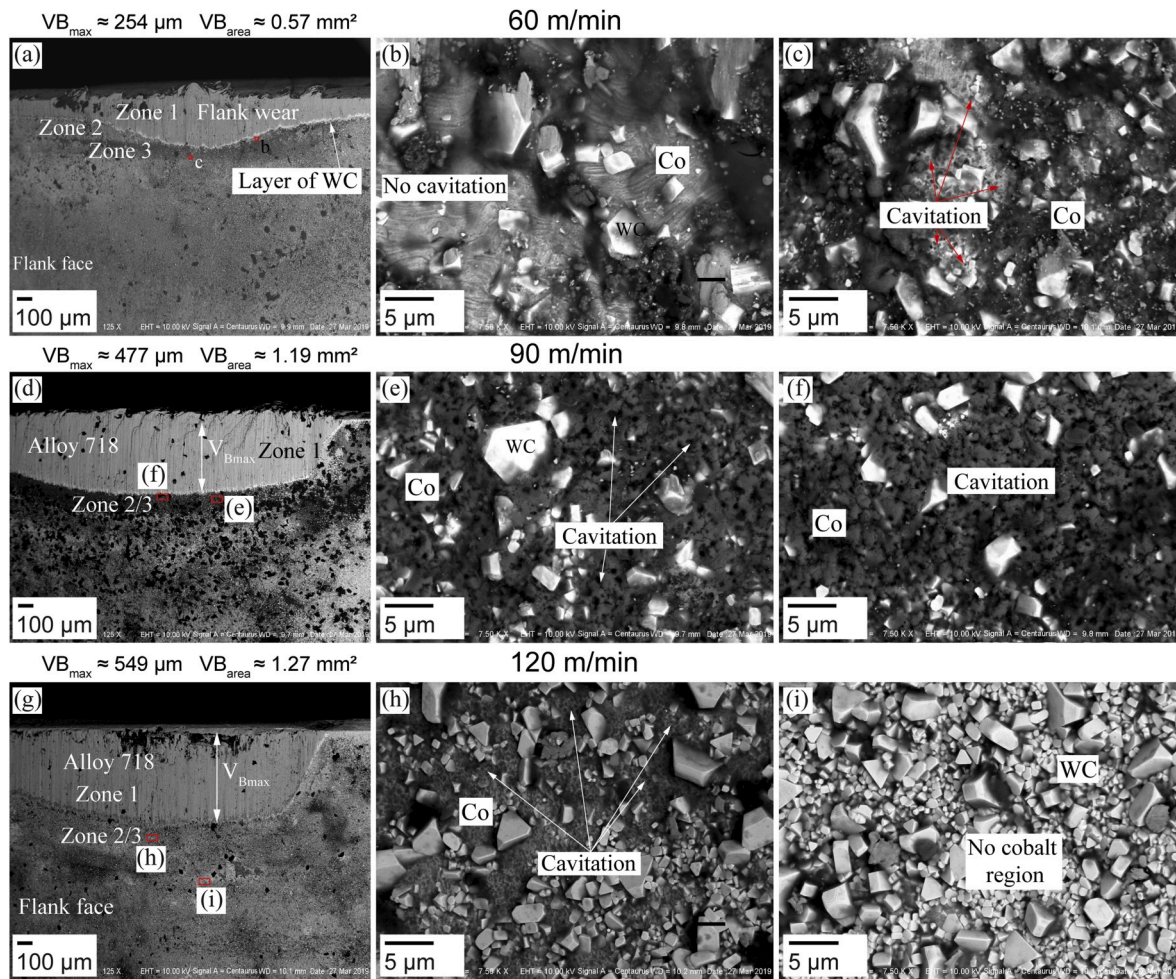


Fig. 13. BSE micrographs of flank faces of the cutting tools, machined at different cutting speeds for Tool-1 (a–c) 60 m/min, (d–f) 90 m/min, and (g–i) 120 m/min.

to the same extent as after the machining tests (see Fig. 9 (c)).

During machining, part of the heat generated in the shear zones dissipates into the tool [32]. As a result, elevated temperatures at the tool surface in the area of coolant impact lead to thermal softening of the Co-layer, see Fig. 10, which is subsequently removed more readily. In contrast, when subjected solely to high-pressure jet impact, the “Co-capping” layer maintains its room temperature strength and can withstand the impact of the coolant jet.

### 3.2. Varying SCL for Tool-1

The BSE images and EDS maps of the flank faces after the machining tests are shown in Fig. 11. All flank wear lands (VB) show adhesion of Alloy 718 workpiece material (see Ni-rich zones in EDS maps). As can be seen, when comparing the micrographs after the respective spiral cutting lengths, a longer tool engagement leads to an increase in flank wear land from about 130 μm after 70 m, to 160 μm after 140 m, and 480 μm after 210 m spiral cutting length, respectively. Furthermore, with increasing spiral cutting length, the shape of the flank wear land changes from uniform (70 and 140 m spiral cutting length) to non-uniform with a local maximum after 210 m.

Even though no contact between workpiece and tool occurred below the flank wear lands, the formation of bright zones can be observed (see BSE images in Fig. 11). The VB value is from one tool measurement. EDS analyses of the respective zones on the tool surfaces reveal a local deficiency of Co, i.e. increased W signal. The removal of Co from the tool surface is caused by erosion due to the impingement of the high-pressure

coolant jets, as shown by the authors in earlier work where the same coolant supply pressures were applied [35].

Further SEM investigations conducted on the selected cutting tool from SCL 70 m focussed on the coolant boiling and cavitation. Fig. 12 shows results of the analysis of the erosion-free area (Zone 2 – no-coolant boiling) in close vicinity to the flank wear land after 70 m spiral cutting length. As indicated in Fig. 12 (a), two areas could be identified where the Co-binder exhibits distinct features (Zone 2 and Zone 3). The transition of one zone to the other is approximated by the line and a higher magnified micrograph is provided in Fig. 12 (b). As seen in Fig. 12 (c), the Co-capping layer in Zone 2 is characterized by signs of initiating wear from the contact with the workpiece. Abrasion marks parallel to the direction of the workpiece movement can be observed while no indications of Co-erosion are visible. In contrast, the Co-binder in Zone 3 (Fig. 12 (d)) clearly shows cavitation pits of sub-micron size. The described distinct Zones 2 and 3 were characteristic for all three conducted tests with 70 m spiral cutting length.

Absence of cavitation erosion signs (Zone 2) shows that no erosion occurred close to the flank wear land. The high temperatures reached during machining seem to have led to rapid vapourization of the coolant, which in turn leads to the formation of a vapour barrier [8,36]. This vapour barrier is then hindering the coolant from reaching closer to the cutting zone, creating a pressure difference along the flank face. Jäger et al. [12] have reported coolant residues below the flank wear lands after machining Alloy 718 under similar cutting conditions. Coolant residues indicate boiling of the coolant during machining which in turn can lead to the proposed vapour barrier phenomenon and



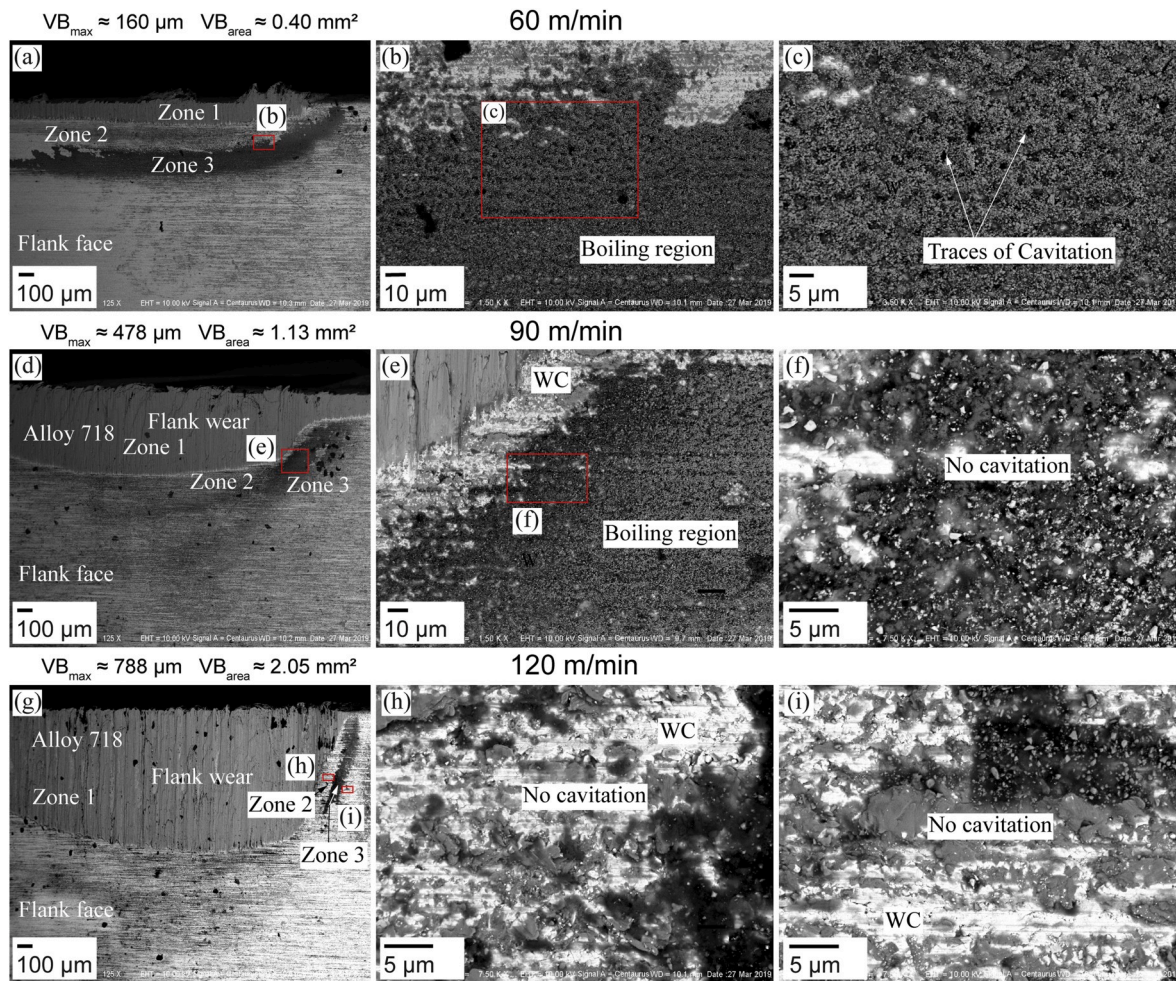


Fig. 14. BSE micrographs of flank faces of the cutting tools machined at different cutting speeds for Tool-2 (a–c) 60 m/min, (d–f) 90 m/min, and (g–i) 120 m/min.

pressure/temperature difference, thus, causing the *cavitation wear* in the form of erosion pits in Zone 3 below the *Leidenfrost* film.

### 3.3. Varying cutting speeds for Tool-1 and Tool-2

The final set of machining experiments were set up to understand the cavitation phenomenon on the same ISO cutting tool (RCMX 12 04 00) but with different surface conditions. Tool-1 (Co on the surface) is our tool of primary interest as compared to Tool-2 (no Co on the surface), due to the grinding of the flank surface, see Fig. 5 (d). The experiments were conducted for increasing cutting speeds (60, 90 and 120 m/min), to have high temperature in the cutting zones and to investigate if there is an influence with coolant boiling and cavitation on the cutting tool with and without cobalt for increased heat and flank wear rate for constant coolant conditions. The selected cutting tools from the Tool-1 category for different cutting speeds were investigated in SEM, see Fig. 13.

The aim was to identify the three different zones along the flank face of the cutting tools. Special focus was put on Zone 2 and Zone 3 where the coolant boiling and cavitation wear were observed. In Zone 1, the flank wear and the adhesion of workpiece material (Alloy 718) is dominant, see Fig. 13 (a, d and g). In case of  $v_c$  60 m/min, higher magnification (7500x) on the area of Zone 2 beneath the flank wear showed the cobalt region without any trace of cavitation, see Fig. 13 (b). Further examination of the area of Zone 3 showed that the cavitation had started on the cobalt surface, but not on the tungsten carbide, Fig. 13 (c). Both the findings are in alignment with previous results of the

authors on cavitation, see subsection 3.1 and 3.2.

For the cutting tools machined at  $v_c$  = 90 and 120 m/min, the zones were different. It was difficult to differentiate the Zone 2 and 3. Moreover, both zones combined together as Zone 2/3 below the flank wear, see Fig. 13 (d and g). This behaviour can be attributed to the increased flank wear that could have led to remove the sign of Zone 2 and Zone 3 and merged the zones compared to the low cutting speed of 60 m/min. Although at the higher  $v_c$  the zone separation was not possible. However, the existence of the cavitation is still visible on both cutting tools below the flank wear in the coolant boiling region, Fig. 13 (e and f and h). At the highest cutting speed of 120 m/min and investigated further away from the Zone 2/3 as shown in Fig. 13 (g), it was possible to reveal that there is no cobalt present, see Fig. 13 (i). This is due to the coolant boiling in combination with high-pressure cooling of 8 MPa on the flank face as discussed in subsection 3.1 and 3.2, see Figs. 9 (c) and Fig. 11. At low  $v_c$  of 60 m/min the coolant boiling and removal of Co were close to the flank wear, at higher  $v_c$  of 120 m/min Co removal and cavitation wear can be found but the locations were shifted.

For a cutting speed of 60 m/min, it was possible to identify Zone 1–3 in Tool 2. The Zone 3, see Fig. 14 (a), was localised (close to the maximum flank wear region) compared to Tool-1 where it was more evenly spread out (see Figs. 6 and 11). SEM was used to investigate the Zone 2 and 3, there were limited traces of cavitation wear on the cutting tool. However, it was possible to identify minor signs of cavitation pits on the Zone 3 at higher magnification (see Fig. 14 (c)). The traces of cavitation wear is limited, while Tool-1 with “cobalt capping” on the surface showed higher visibility of cavitation.

Zone 2 and 3 were located similarly on the tools used for  $v_c$  90 and 120 m/min. Zone 3 was not spread over the entire flank wear region but was rather localised (maximum flank wear region). However, the traces started to reduce, see Fig. 14 (d and g). There was a small region of Zone 2 and Zone 3 for both cutting speeds. The cutting tools were examined at different locations on the flank surface and there was no trace of cavitation wear. Selected regions of interest are shown in Fig. 14 (e and f, h and i). The absence of cavitation wear may be due to the influence of temperature on mechanical properties of Co. Reported hardness values as a function of temperature are shown in Fig. 10. Since the Co-binder in WC-Co tools contains some dissolved W and C [37], alloyed Co is shown in addition to pure Co. Throughout the entire measured temperature range, alloyed Co consistently shows higher hardness as compared to pure Co. This can be explained by the solid solution strengthening effect provided by the dissolved W and C. While only half of the room temperature hardness of pure Co is retained at 500 °C, the hardness loss is less pronounced for the alloyed Co. Still, irrespective of alloying, the hardness decreases steadily as the temperature increases and hence enables the occurrence of erosion pits as *cavitation wear* in combination with the impact of the high-pressure coolant jets during machining in case of Tool-1 (Co on the surface). However, coolant jet and coolant boiling do not have a strong influence on the Tool-2 (no Co surface), since WC is a stronger and harder compound than Co in spite of a rise in temperature.

In machining of Alloy 718, one of the emphasized research areas is tool wear rate and wear mechanisms. The commonly found wear mechanisms during machining this material are adhesion (build-up-edge/material), abrasion (flank wear), diffusion (crater wear), notch wear, plastic deformation, and cracking of the tool. Apart from these wear types and mechanisms which have been recognized for decades, this research work has shown that by adding the high-pressure coolant when machining Alloy 718 “without the knowledge of coolant vapour pressure”, could lead to forming the “Leidenfrost” film and the “coolant-boiling” phenomenon. The presence of these two phenomena acting on the tool flank led to the finding of “Cavitation Wear” and its existence “as a new wear mechanism” on the WC cutting tool (Tool-1).

#### 4. Conclusion

This research work led to the discovery of a wear mechanism in machining previously not reported: “Cavitation Wear”. This type of wear is closely related to the application of coolant media under high-pressure on the flank surface of a tool (Tool-1 (cobalt on the surface)).

In case no flank cooling is used, no sign of cavitation wear can be found on the cutting tool.

The occurrence of cavitation wear is linked to the Leidenfrost effect that acts as the barrier for the coolant, therefore likely to create a pressure/temperature difference along the flank surface which enables the occurrence of “Cavitation Wear” and the formation of cavitation pits. The signs of cavitation were found beneath the flank wear region, mostly in the area of coolant boiling.

An increase in flank pressure resulted in a corresponding decrease in  $VB_{max}$  and  $VB_{area}$  and the coolant-boiling region followed the flank wear land, moving closer to the cutting edge.

To avoid the “Leidenfrost” effect, causing the coolant to boil and “Cavitation wear” to occur, it is important to control the cutting temperature. This can be achieved through either or both of the following:

- Adjusting the cutting speed to control the temperature of the tool to stay below the “Leidenfrost” point of the coolant (preferably in the nucleate boiling region).
- Adjusting the media pressure directed towards the tool flank in order to stay above the vapour pressure of the coolant for the corresponding cutting temperature.

#### Declaration of competing interest

The authors declare that they have no known competing financial interests or personal relationships that could have appeared to influence the work reported in this paper.

#### Acknowledgements

The authors would like to thank Västra Götalandsregionen for funding in association with the PROSAM project. Special thanks go to Andreas Gustafsson at University West and Andreas Lindberg at GKN Aerospace Engine Systems AB for help with experiments, Fabian Hanning from Chalmers University of Technology for help with SEM. The authors gratefully acknowledge the financial support for open access publishing from the corporate research school SiCoMaP, funded by the Stiftelsen för Kunskaps och Kompetensutveckling (Knowledge Foundation), Dnr: 20140130.

“We would like to thank and show the deepest gratitude to the health workers fighting against “Corona Virus” and support future research in epidemic diseases”.

#### References

- [1] E.O. Ezugwu, J. Bonney, Y. Yamane, An overview of the machinability of aeroengine alloys, *J. Mater. Process. Technol.* 134 (2) (Mar. 2003) 233–253, [https://doi.org/10.1016/S0924-0136\(02\)01042-7](https://doi.org/10.1016/S0924-0136(02)01042-7).
- [2] E. Rahim, N. Warap, Z. Mohid, in: M. Aliofkhaezai (Ed.), “Thermal-Assisted Machining of Nickel-Based Alloy,” in *Superalloys*, InTech, 2015.
- [3] F. Klocke, B. Döbbeler, T. Lakner, Influence of the coolant nozzle orientation and size on the tool temperature under high-pressure coolant supply using an analogy test bench, *Prod. Eng.* 12 (3) (Jun. 2018) 473–480, <https://doi.org/10.1007/s11740-018-0823-2>.
- [4] A. Suárez, L.N.L. de Lacalle, R. Polvorosa, F. Veiga, A. Wretland, Effects of high-pressure cooling on the wear patterns on turning inserts used on alloy IN718, *Mater. Manuf. Process.* (Oct. 2016), <https://doi.org/10.1080/10426914.2016.1244838>, 0, no. ja, p. null.
- [5] A.U.H. Mohsan, Z. Liu, X. Ren, W. Liu, “Influences of cutting fluid conditions and cutting parameters on surface integrity of Inconel 718 under high-pressure jet-assisted machining (HPJAM), *Lubric. Sci.* 30 (6) (Oct. 2018) 269–284, <https://doi.org/10.1002/ls.1418>.
- [6] N. Tamil Alagan, P. Hoier, P. Zeman, U. Klement, T. Beno, A. Wretland, Effects of High-Pressure Cooling in the Flank and Rake Faces of WC Tool on the Tool Wear Mechanism and Process Conditions in Turning of Alloy 718, *Wear*, Jun. 2019, <https://doi.org/10.1016/j.wear.2019.05.037>.
- [7] R.J.S. Pigott, A.T. Colwell, Hi-jet system for increasing tool life, *SAE Tech. Pap.* (1952), <https://doi.org/10.4271/520254>.
- [8] E.O. Ezugwu, J. Bonney, Effect of high-pressure coolant supply when machining nickel-base, Inconel 718, alloy with coated carbide tools, *J. Mater. Process. Technol.* 153 (154) (Nov. 2004) 1045–1050, <https://doi.org/10.1016/j.jmatprot.2004.04.329>.
- [9] R.B. da Silva, Á.R. Machado, E.O. Ezugwu, J. Bonney, W.F. Sales, “Tool life and wear mechanisms in high speed machining of Ti–6Al–4V alloy with PCD tools under various coolant pressures, *J. Mater. Process. Technol.* 213 (8) (Aug. 2013) 1459–1464, <https://doi.org/10.1016/j.jmatprot.2013.03.008>.
- [10] A. Krämer, F. Klocke, H. Sangermann, D. Lung, Influence of the lubricoolant strategy on thermo-mechanical tool load, *CIRP J. Manuf. Sci. Technol.* 7 (1) (Jan. 2014) 40–47, <https://doi.org/10.1016/j.cirpj.2013.09.001>.
- [11] F. Klocke, D. Lung, T. Cayli, B. Döbbeler, H. Sangermann, Evaluation of energy efficiency in cutting aerospace materials with high-pressure cooling lubricant supply, *Int. J. Precis. Eng. Manuf.* 15 (6) (Jun. 2014) 1179–1185, <https://doi.org/10.1007/s12541-014-0454-2>.
- [12] H. Jäger, N.T. Alagan, J. Holmberg, T. Beno, A. Wretland, EDS analysis of flank wear and surface integrity in machining of alloy 718 with forced coolant application, *Procedia CIRP* 45 (2016) 271–274, <https://doi.org/10.1016/j.procir.2016.02.144>.
- [13] Yunus A. Çengel, *Heat and Mass Transfer: Fundamentals and Applications*, 5th Ed. In SI Units, McGraw-Hill, New York, 2015.
- [14] N. Tamil Alagan, T. Beno, P. Hoier, U. Klement, A. Wretland, Influence of surface features for increased heat dissipation on tool wear, *Materials* 11 (5) (Apr. 2018) 664, <https://doi.org/10.3390/ma11050664>.
- [15] K. Sørby, K. Tønnessen, High-pressure cooling of face-grooving operations in Ti6Al4V, *Proc. Inst. Mech. Eng. Part B J. Eng. Manuf.* 220 (10) (2006) 1621–1627, <https://doi.org/10.1243/09544054JEM474>.
- [16] J.-P. Franc, J.-M. Michel, *Fundamentals of Cavitation*, Springer Netherlands, 2005.
- [17] F. Klocke, H. Sangermann, A. Krämer, D. Lung, Influence of a high-pressure lubricoolant supply on thermo-mechanical tool load and tool wear behaviour in the turning of aerospace materials, *Proc. Inst. Mech. Eng. Part B J. Eng. Manuf.* 225 (1) (Jan. 2011) 52–61, <https://doi.org/10.1177/09544054JEM2082>.

- [18] Phillip Eisenberg, On the Mechanism and Prevention of Cavitation, Navy Dept., David W. Taylor Model Basin, Washington, 1950, 712.
- [19] Defense Technical Information Center, DTIC ADP012072: Introduction to Cavitation and Supercavitation, 2001.
- [20] A. Peters, H. Sagar, U. Lantermann, O. el Mactar, Numerical modelling and prediction of cavitation erosion, *Wear* 338 (339) (Sep. 2015) 189–201, <https://doi.org/10.1016/j.wear.2015.06.009>.
- [21] E.C. Fitch, Proactive Maintenance for Mechanical Systems, Elsevier Science & Technology, Kent, UNITED KINGDOM, 1992.
- [22] D.C. Wiggert, C.S. Martin, H. Medlarz, Cavitation Damage Mechanisms: Review of Literature, Georgia Inst of Tech Atlanta School of Civil Engineering, Feb. 1980.
- [23] E.C. Fitch, Hydraulic cavitation wear explained and illustrated, 23-Apr-2014. [Online]. Available, <https://www.machinerylubrication.com/Read/380/cavitation-wear-hydraulic>. (Accessed 1 March 2019).
- [24] C.E. Brennen, Fundamentals of Multiphase Flow, Cambridge University Press, 2005.
- [25] Y.F. Ronald, Cavitation, World Scientific, 1999.
- [26] P. Hoier, U. Klement, N. Tamil Alagan, T. Beno, A. Wretland, Flank wear characteristics of WC-Co tools when turning Alloy 718 with high-pressure coolant supply, *J. Manuf. Process.* 30 (Dec. 2017) 116–123, <https://doi.org/10.1016/j.jmapro.2017.09.017>.
- [27] R. Danzl, F. Helml, P. Rolland, S. Scherer, Geometry and volume measurement of worn cutting tools with an optical surface metrology device, in: *In Transverse Disciplines In Metrology*, John Wiley & Sons, Ltd, 2010, pp. 373–382.
- [28] Iso 3685:1993, Tool-life Testing with Single-point Turning Tools-ISO 3685:1993, 2011.
- [29] D.S. Janisch, W. Lengauer, K. Rödiger, K. Dreyer, H. van den Berg, Cobalt capping: why is sintered hardmetal sometimes covered with binder? *Int. J. Refract. Metals Hard Mater.* 28 (3) (May 2010) 466–471, <https://doi.org/10.1016/j.ijrmhm.2010.02.006>.
- [30] E. Sachet, W.D. Schubert, G. Mühlbauer, J. Yukimura, Y. Kubo, On the formation and in situ observation of thin surface layers of cobalt on sintered cemented carbides, *Int. J. Refract. Metals Hard Mater.* 31 (Mar. 2012) 96–108, <https://doi.org/10.1016/j.ijrmhm.2011.09.012>.
- [31] Vaporous and gaseous cavitation, Aquatherm, Newsletter 2 (2017).
- [32] F. Klocke, Manufacturing Processes 1: Cutting, Springer-Verlag, Berlin Heidelberg, 2011.
- [33] W. Betteridge, Cobalt and its Alloys, E. Horwood, 1982.
- [34] M. Lee, High temperature hardness of tungsten carbide, *Metall. Trans. A* 14 (8) (1983) 1625–1629, <https://doi.org/10.1007/BF02654390>.
- [35] P. Hoier, U. Klement, N. Tamil Alagan, T. Beno, A. Wretland, Characterization of tool wear when machining Alloy 718 with high pressure cooling using conventional and surface-modified WC-Co tools, *Springer J. Superhard Mater.* 39 (2017) 178–185, <https://doi.org/10.3103/S1063457617030054>.
- [36] F. Klocke, D. Lung, A. Krämer, T. Cayli, H. Sangermann, Potential of modern lubricoolant strategies on cutting performance, *Key Eng. Mater.* 554 (2013) 2062–2071. <https://doi.org/10.4028/www.scientific.net/KEM.554-557.2062>.
- [37] H.E. Exner, Physical and chemical nature of cemented carbides, *Int. Met. Rev.* 24 (1) (Jan. 1979) 149–173, <https://doi.org/10.1179/imtr.1979.24.1.149>.